

ROBERT W. ZIMMERMAN
ADRIANA PALUSZNY

FLUID FLOW IN

**FRACTURED
ROCKS**



WILEY

Fluid Flow in Fractured Rocks

Fluid Flow in Fractured Rocks

Robert W. Zimmerman and Adriana Paluszny

Department of Earth Science and Engineering
Imperial College London
London, UK

WILEY

This edition first published 2024
© 2024 John Wiley & Sons Ltd.

All rights reserved. No part of this publication may be reproduced, stored in a retrieval system, or transmitted, in any form or by any means, electronic, mechanical, photocopying, recording or otherwise, except as permitted by law. Advice on how to obtain permission to reuse material from this title is available at <http://www.wiley.com/go/permissions>.

The right of Robert W. Zimmerman and Adriana Paluszny to be identified as the authors of this work has been asserted in accordance with law.

Registered Offices

John Wiley & Sons, Inc., 111 River Street, Hoboken, NJ 07030, USA

John Wiley & Sons Ltd, The Atrium, Southern Gate, Chichester, West Sussex, PO19 8SQ, UK

For details of our global editorial offices, customer services, and more information about Wiley products visit us at www.wiley.com.

Wiley also publishes its books in a variety of electronic formats and by print-on-demand. Some content that appears in standard print versions of this book may not be available in other formats.

Trademarks: Wiley and the Wiley logo are trademarks or registered trademarks of John Wiley & Sons, Inc. and/or its affiliates in the United States and other countries and may not be used without written permission. All other trademarks are the property of their respective owners. John Wiley & Sons, Inc. is not associated with any product or vendor mentioned in this book.

Limit of Liability/Disclaimer of Warranty

While the publisher and authors have used their best efforts in preparing this work, they make no representations or warranties with respect to the accuracy or completeness of the contents of this work and specifically disclaim all warranties, including without limitation any implied warranties of merchantability or fitness for a particular purpose. No warranty may be created or extended by sales representatives, written sales materials or promotional statements for this work. This work is sold with the understanding that the publisher is not engaged in rendering professional services. The advice and strategies contained herein may not be suitable for your situation. You should consult with a specialist where appropriate. The fact that an organization, website, or product is referred to in this work as a citation and/or potential source of further information does not mean that the publisher and authors endorse the information or services the organization, website, or product may provide or recommendations it may make. Further, readers should be aware that websites listed in this work may have changed or disappeared between when this work was written and when it is read. Neither the publisher nor authors shall be liable for any loss of profit or any other commercial damages, including but not limited to special, incidental, consequential, or other damages.

Library of Congress Cataloging-in-Publication Data

Names: Zimmerman, Robert Wayne, author. | Paluszny, Adriana, author.

Title: Fluid flow in fractured rocks / Robert W. Zimmerman and Adriana Paluszny.

Description: Hoboken, NJ : Wiley, 2024. | Includes index.

Identifiers: LCCN 2023039657 (print) | LCCN 2023039658 (ebook) | ISBN 9781119248019 (cloth) | ISBN 9781119248033 (adobe pdf) | ISBN 9781119248026 (epub)

Subjects: LCSH: Rocks—Fracture. | Fluid dynamics.

Classification: LCC TA706 .Z56 2024 (print) | LCC TA706 (ebook) | DDC 620.1/064—dc23/eng/20230909

LC record available at <https://lcn.loc.gov/2023039657>

LC ebook record available at <https://lcn.loc.gov/2023039658>

Cover image: © ROMAN DZIUBALO/Shutterstock

Cover design: Wiley

Set in 9.5/12.5pt STIXTwoText by Straive, Chennai, India

Contents

Preface *ix*

Author Biographies *xi*

About the Companion Website *xiii*

1 Genesis and Morphology of Fractures in Rock *1*

1.1 What Are Fractures, and Why Are They Important? *1*

1.2 Formation of Fractures in Rock *2*

1.3 Morphology of Single Fractures *5*

1.4 Morphology of Fracture Networks *14*

Problems *20*

References *21*

2 Fluid Flow in a Single Fracture *27*

2.1 Introduction *27*

2.2 The Navier–Stokes Equations and the Cubic Law *28*

2.3 The Stokes Equations *32*

2.4 The Reynolds Lubrication Equation *36*

2.5 Effect of Contact Area *41*

2.6 Accuracy of the Lubrication Model *43*

2.7 Fracture in a Permeable Matrix *46*

2.8 Fracture Filled with Porous or Granular Material *49*

Problems *52*

References *52*

3 Effect of Stress on Fracture Transmissivity *57*

3.1 Introduction *57*

3.2 The Effect of Normal Stress on Fracture Deformation *58*

3.3 Models for the Normal Stiffness of Rock Fractures *60*

3.4 “Row of Elliptical Voids” Model for Fracture Transmissivity *63*

3.5 Relation Between Transmissivity and Mean Aperture During Normal Compression *68*

- 3.6 Effect of Shear Deformation on Fracture Transmissivity Problems 70
References 72

- 4 Fluid Flow Through Fractures at Moderate to High Reynolds Numbers 75**
 - 4.1 Introduction 75
 - 4.2 Approximate Analytical Solution for a Sinusoidal Fracture Aperture 76
 - 4.3 Weak Inertia Regime and Forchheimer Regime 77
 - 4.4 Verification of the Weak Inertia and Forchheimer Regimes 80
 - 4.5 Experimental Data on Fluid Flow at Moderate to High Reynolds Numbers 84
 - 4.6 Flow of Compressible Gases Through Fractures Problems 85
References 88

- 5 Thermo-Hydro-Chemical-Mechanical Effects on Fracture Transmissivity 91**
 - 5.1 Introduction 91
 - 5.2 Fracture Contact 92
 - 5.3 Pressure Dissolution 94
 - 5.4 Diffusion Rates 97
 - 5.5 Solute Precipitation 98
 - 5.6 Aperture Changes 99
 - 5.7 Relationship Between Aperture, Contact Fraction, and Transmissivity 101
 - 5.8 Numerical Simulations of Pressure Solution 103
 - 5.9 Lehner–Leroy Model for Pressure Dissolution 104
 - 5.10 Bernabé–Evans Model for Pressure Dissolution 106
 - 5.11 Dissolution and Precipitation in Open and Closed Systems Problems 109
References 110

- 6 Solute Transport in a Single Fracture 113**
 - 6.1 Introduction 113
 - 6.2 Advection–Diffusion Equation 114
 - 6.3 Taylor–Aris Problem in a Uniform Channel 118
 - 6.4 Influence of Fracture Morphology on Solute Transport 121
 - 6.5 Non-Fickian Transport in Rock Fractures 123
 - 6.6 Influence of Adsorption, Matrix Diffusion, and Radioactive Decay Problems 128
References 128

- 7 Analytical Models for the Permeability of a Fractured Rock Mass 133**
 - 7.1 Introduction 133
 - 7.2 Snow’s Model of Planar Fractures of Infinite Extent in an Impermeable Matrix 134

7.3	Upper and Lower Bounds on the Effective Permeability	136
7.4	Spheroidal Inclusion Model of a Fractured Rock Mass	137
7.5	Effective Permeability in the Regime $\alpha/\kappa \ll 1$	140
7.6	Effective Permeability in the Regime $\alpha/\kappa \gg 1$	142
7.7	Semi-empirical Model of Mourzenko <i>et al.</i>	144
	Problems	145
	References	146
8	Fluid Flow in Geologically Realistic Fracture Networks	149
8.1	Introduction	149
8.2	Stochastically Generated Fracture Networks	150
8.3	Geomechanically Generated Fracture Networks	152
8.4	Intersections and Connectivity in Fracture Networks	155
8.5	Fracture Apertures in Discrete Fracture Networks	156
8.6	Numerical Computation of Fractured Rock Mass Permeability	159
8.7	Effect of Fracture Density on Equivalent Permeability	163
8.8	Effect of <i>In Situ</i> Stresses on Equivalent Permeability	166
8.9	Channels and Preferential Flow Pathways	170
	Problems	172
	References	173
9	Dual-Porosity Models for Fractured-Porous Rocks	177
9.1	Introduction	177
9.2	Pressure Diffusion Equation for the Fractured Continuum	178
9.3	Fracture/Matrix Fluid Interaction Term	180
9.4	Equation for the Evolution of the Mean Pressure in the Matrix Blocks	182
9.5	Warren–Root Solution for Flow to a Well in a Dual-Porosity Medium	184
9.6	Fully Transient model for Matrix-to-Fracture Flow	188
9.7	Nonlinear Matrix-Fracture Transfer Model	190
9.8	Multi-Phase Flow, Gravity Effects, and Other Extensions	193
	Problems	195
	References	196
10	Matrix Block Shape Factors	199
10.1	Introduction	199
10.2	Approaches to Choosing the Shape Factor	200
10.3	Some Specific Results and General Theorems	202
10.4	Upper and Lower Bounds on the Shape Factor	203
10.5	Methodology for Numerical Calculation of the Shape Factor	204
10.6	Scaling Laws for Irregularly Shaped Matrix Blocks	207
10.7	Shape Factor Under Constant-Flux Boundary Conditions	209
10.8	Constant-Flux Shape Factor for a Brick-like Matrix Block	213
	Problems	215
	References	215

11	Solute Transport in Fractured Rock Masses	219
11.1	Introduction	219
11.2	Advection–Dispersion and Solute Transport Equations	220
11.3	Numerical Solution of the Advection–Dispersion and Solute Transport Equations	222
11.4	Non-Fickian Transport	226
11.5	Channel Models	227
11.6	Particle Tracking Methods	230
11.7	Continuous Time Random Walk Approach	232
11.8	Effects of Matrix Permeability	234
11.9	Effects of <i>In Situ</i> Stresses	235
	Problems	236
	References	237
12	Two-Phase Flow in Fractured Rocks	241
12.1	Introduction	241
12.2	Basic Concepts of Two-Phase Flow	242
12.3	Pruess–Tsang Model of Two-Phase Flow in a Single Fracture	246
12.4	Other Models and Observations of Two-Phase Flow in a Single Fracture	248
12.5	Dual-Porosity and Dual-Permeability Models for Two-Phase Flow	251
12.6	Discrete-Fracture Network Models for Two-Phase Flow in Fractured Rock Masses	254
	Problems	256
	References	256
	List of Symbols	259
	Index	265

Preface

Several well-regarded books have been written over the years on fluid flow in porous media and subsurface hydrology. However, it is now recognized that *fractured* rocks are ubiquitous in the subsurface, and that several issues that arise during fluid flow and transport through fractured rocks are distinct from their analogues in non-fractured porous media. Moreover, flow and transport through fractured rocks are of great importance in many technological areas, such as, for example, energy production from geothermal or hydrocarbon reservoirs, subsurface nuclear waste disposal, carbon sequestration, and contaminant remediation. Hence, there is a need for a monograph/textbook that provides a thorough, rigorous, and authoritative introduction to this topic. Our aim in writing this book has been to address this need.

This book was intended to be written in sufficient detail so as to provide a rigorous and broad introduction to the field of fluid flow through fractured rocks. It is intended for readers with interests in hydrogeology, hydrology, water resources, structural geology, reservoir engineering, underground waste disposal, or other fields that involve the flow of fluids through fractured rock masses. To the extent possible, the mathematical models developed and discussed in the book are compared to experimental or field data or validated/tested against numerical simulations. The book contains 157 individual figures, of which 39 are either images of real fractures or contain actual laboratory or field data.

Chapter 1 introduces the geomechanical background to the nucleation and growth of fractures in rock and the multi-scale characterization of their geometric traits, such as aperture, length, roughness, and density. Chapter 2 provides a rigorous treatment of the mathematics of fluid flow through a single rock fracture, starting with the Navier–Stokes equations and carefully explaining the conditions under which these equations can be replaced by the simpler Stokes equations or Reynolds lubrication equation. The effects of normal and shear stresses on the transmissivity of a rock fracture are discussed in Chapter 3. Chapter 4 discusses the effects of inertia on fluid flow through a fracture and the resulting deviations from a Darcy-like linear relation between pressure drop and flowrate. Some of the coupled thermal, hydraulic, mechanical, and chemical interactions that may alter the transmissivity of a single fracture are described in Chapter 5. Chapter 6 introduces the concept of solute transport through single fractures and presents some models for the advection and dispersion of solutes.

Whereas most of the first six chapters focus on flow and transport through a single fracture, the second half of the book focuses on the behavior of fracture networks and fractured

rock masses. Chapter 7 presents some analytical models for the macroscopic-scale permeability of porous/fractured rocks. Chapter 8 discusses various approaches to the numerical modeling of fluid flow through geologically realistic fracture networks and fractured rock masses. Chapter 9 presents “dual-porosity” models for fractured-porous media, starting from the classical model developed by Barenblatt and his collaborators. Chapter 10 then gives a detailed treatment of the matrix block shape factors that are crucial ingredients in dual-porosity models for both flow and transport. Various models for solute transport through fracture networks and fractured rock masses, both “Fickian” and “non-Fickian,” are discussed in Chapter 11. Finally, Chapter 12 briefly discusses two-phase flow in single fractures and fractured rocks.

Although this book might be classified as a monograph, it is hoped that it can also serve as a textbook for master’s-level or advanced undergraduate courses. For this purpose, several problems have been given at the end of each chapter. Some of the problems ask for a mathematical derivation of an equation that may have been presented in the text without a detailed derivation. Other problems ask for analysis of data or further analysis and/or application of some of the mathematical models presented in the book.

This book is intended to be self-contained. Most of the mathematical derivations are presented in sufficient detail so as not to require the reader to refer to the original sources. Nevertheless, extensive reference is made to important papers, theses, and books that have made contributions to the field and/or contain relevant information. The references in each chapter have been collected at the end of that chapter rather than in a single reference list, for the convenience of the reader.

Equations are numbered consecutively within each chapter, so that, for example, “Eq. (5.7)” denotes the seventh equation in Chapter 5. Tables and figures are also numbered in this same manner, *i.e.*, numbering is not restarted within each section of a chapter. All symbols and variables are defined in the text, as soon as they are first used. When a variable is first defined, its “dimensions” are listed in brackets, in terms of the SI units that would typically be used for that variable, rather than in terms of the “Mass-Length-Time” convention. Efforts have been made to adhere to a consistent nomenclature, sometimes at the cost of not using the same notation as was used in the original sources of some of the equations. The large number of variables mentioned in the book made it unavoidable that some letters be used to denote different properties in different chapters. To avoid confusion, a single List of Symbols has been included at the end of the book, which in particular explains the meaning of those symbols that are used for different purposes in different chapters.

To aid in the use of this book as a textbook, all figures can be freely downloaded (see ‘About the Companion Page’ on page xiii). The authors welcome feedback from readers or users of this book, including notification of any errors that may be detected.

London, UK
October 2023

Robert W. Zimmerman
Adriana Paluszny

Author Biographies

Robert W. Zimmerman earned BS and MS degrees from Columbia University and a PhD from the University of California at Berkeley. He has been a staff scientist at the Lawrence Berkeley National Laboratory, the Head of the Division of Engineering Geology and Geophysics at the Royal Institute of Technology in Stockholm, and is currently a Professor of Rock Mechanics at Imperial College in London. He has been the Editor-in-Chief of the *International Journal of Rock Mechanics and Mining Sciences* since 2007 and is co-author, with J.C. Jaeger and N.G.W. Cook, of *Fundamentals of Rock Mechanics*, 4th ed. (Wiley-Blackwell, 2007).

Adriana Paluszny earned an Ing. degree *cum laude* in Computational Engineering from Universidad Simón Bolívar in Caracas, Venezuela, and a PhD in Computational Geomechanics from Imperial College. She is an Associate Editor of the *Journal of Geophysical Research: Solid Earth*, was the inaugural recipient of the Chin-Fu Tsang Coupled Processes Award, and is the main developer of the Imperial College Geomechanics Toolkit. She is currently a Royal Society University Research Fellow, and a Reader in Computational Geomechanics at Imperial College in London.

To my children

Adriana Paluszny
London, UK
28 November 2023

About the Companion Website

This book is accompanied by a companion website.

www.wiley.com/go/zimmerman/fluidflowinfracturedrocks



This website include: Figures from the book

1

Genesis and Morphology of Fractures in Rock

1.1 What Are Fractures, and Why Are They Important?

Fractures are discontinuities in the mechanical integrity of brittle Earth materials. They break the mechanical continuity of the medium and provide high-speed conduits for fluids to flow throughout the subsurface. Consequently, they are crucial to understanding how fluids migrate in the subsurface. Fractures play a key role in controlling how otherwise low-permeability media can allow the migration of fluids through the subsurface. Therefore, fractures can effectively provide access to natural resources such as water, gas, minerals, and geothermal energy. In some cases, fractures may provide unwanted migration paths for stored fluids by breaking geological seals and enabling fluid mixing, leading to the pollution of drinking water resources. In other situations, fractures can facilitate fluid migration, lead to undesirable consequences such as induced seismicity, or possibly compromise the long-term subsurface disposal of hazardous waste.

“Fracture” is a general term that can be used to describe discontinuities formed by extension or shear, including cracks, joints, and faults. Fractures can form veins as a result of long-term mineralization or can be filled by the intrusion of another material, such as magma, to form dykes or other structures (Pollard and Aydin, 1988). Fractures rarely appear as stand-alone features in the subsurface, as deformation of brittle bodies often leads to the creation of multiple simultaneous breaks in rocks, resulting in several superimposed fractures and fault patterns that form complex multi-scale systems. These discontinuities in the rock matrix influence mechanical properties and the conduction of fluids through most low-permeability media. Fractures are discontinuities with imperfect surfaces, which represent weakness in a mechanical sense. Terms related to the description of these discontinuities can be classified into geological, geometric, topological, and mechanical (Peacock *et al.*, 2016). Fractures in rocks have a geological interpretation, usually tied to their setting, geometry, and chemical composition. Connectivity dictates the topological relationship between fractures, and mechanical deformation further changes a fracture’s properties and its form.

From the mechanical point of view, fractures limit the strength of a rock mass, mostly due to a lack of cohesion. From the point of view of fluid flow, they represent preferred conduits for flow since the aperture of a fracture is usually much larger than the pores of the host rock. Pre-existing fractures can be exploited, as they can channel flow through a reservoir, and their observation can serve to provide clues about how rocks conducted fluids

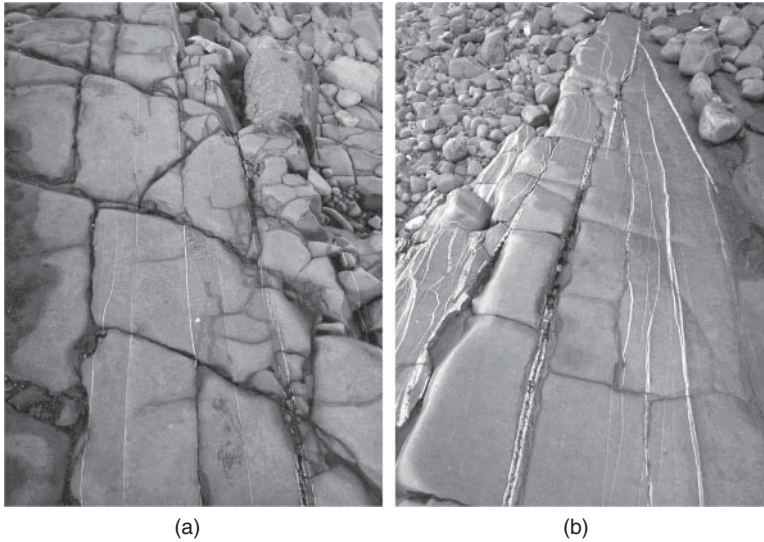


Figure 1.1 (a) Fractures at the centimeter and meter scales cross-cut each other to form complex multi-scale patterns. (b) Fractures in limestone exposed in Somerset, UK.

in the past. Fractures can also be induced or enhanced to increase local fluid flow in order to turn an otherwise impermeable rock into a permeable medium. Figure 1.1 shows some examples of fractures that were formed due to folding of layered limestones off the coast of Somerset, UK.

Isolating the behavior of fractures in a rock formation often represents a bounding scenario for safety cases in evaluating the integrity of underground waste repositories. In the field of geological carbon dioxide storage, for example, a project is commonly considered unsafe if injection-induced overpressure may cause slip along fractures. In geological nuclear waste disposal, the limiting case is often considered to be one in which fluid flow occurs only within the connected system of fractures and whether the ensuing radionuclide transport within this network exceeds some threshold. It follows that fractures are a logical point at which to start investigations on the impact that human interference has on an embedded geological setting, in terms of its mechanical and hydraulic properties.

1.2 Formation of Fractures in Rock

Materials that are quasi-brittle, such as most rocks in the upper crust of the Earth, are subjected to stresses resulting from gravity as well as a variety of local and regional stresses such as tectonic stresses, burial, uplifting, and folding, along with chemical, thermal, and fluid flow-related stresses. As a result, rocks deform in several stages. First, they develop micro-cracks that occur on a small scale, often along the boundaries of individual grains of a rock. These micro-cracks start to grow and form preferential paths which, when aligned, become material flaws. Flaws induce stress concentrations at their tips, the leading edge

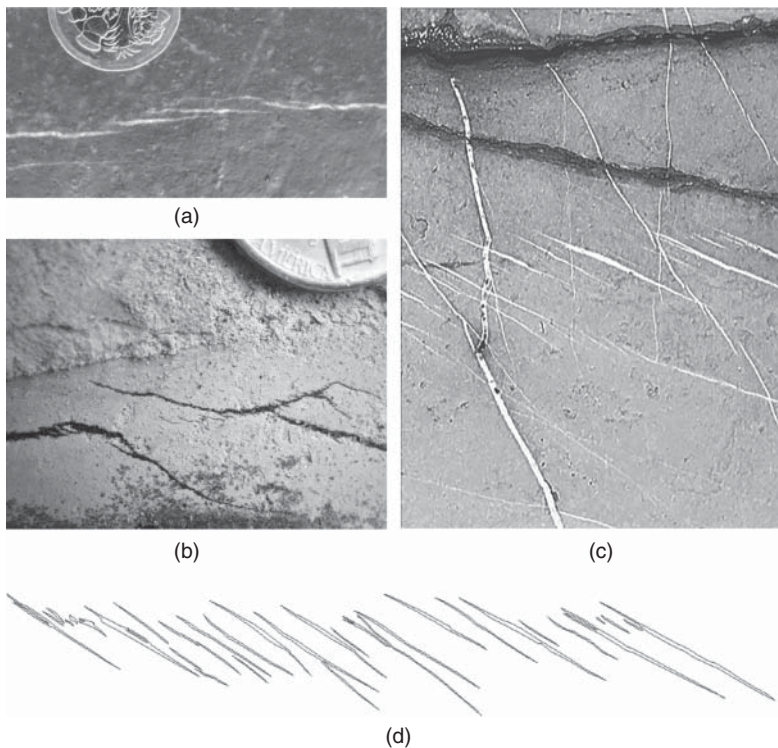


Figure 1.2 Fractures at the centimeter and millimeter scales in (a) and (c) limestone and (b) shale, respectively. The small fractures in (b) arise in one of the shale outcrops that cap the shallow Orcutt oil field in California, USA. In (a) and (c), fractures are filled with calcite, and in (b), fractures are tinted with naturally migrating hydrocarbon. The tracing of the fracture pattern in (c) for aperture quantification is shown in (d).

of the shape of the fracture, causing them to grow and extend into other areas of the rock. This self-organization occurs at larger and larger scales, up to the kilometer scale or larger. During this process, micro-fractures continue to form at different scales around fracture tips, as a result of stress field interactions, as well as other nonlocal chemical and thermal processes. This results in fracture growth across multiple scales to accommodate the ubiquitous deformation of the subsurface. Figure 1.2 shows several examples of interacting fractures. In all of these cases, the fractures are filled with material that delineates their shape, which is not always the case in the subsurface, but is convenient for visualization and interpretation purposes.

During or after fracture growth, the opposing fracture walls can be displaced in relation to one another. Under tension, fracture walls move directly apart (mode I), creating “thickness” or “aperture.” Under shear (modes II and III), fracture walls slide against each other in a direction perpendicular to or parallel to the tip of the crack, respectively. A specific case of a displaced fracture is a “fault,” which exhibits relative displacement of its walls and can appear under normal or shear deformation at scales that span from the centimeter up to the kilometer scale (Gudmundsson, 2000).

Fractures localize across large scales, usually along a preferential plane, and eventually link together to form larger features. From this moment onwards, stress is preferentially concentrated at the tips of the newly formed high-aspect ratio fracture, and growth drives the formation and linkage of larger discontinuities. As rocks are subjected to a variety of mechanical, hydraulic, thermal, and chemical changes over millions of years, many of these flaws form around pre-existing weaknesses in the matrix, pockets of low-integrity rock matrix that have resulted from localized processes. Heterogeneities leading to micro-fractures have been found to follow a Gaussian size distribution (Underwood, 1970), and in brittle rocks, they often appear as thin, penny-shaped microcavities distributed across the matrix (Herrmann, 1990).

Computerized tomography (CT) can reveal fractures with apertures up to five times smaller than the resolution provided by a scanner (Fig. 1.3), due to the strong density contrast between rock and gas/air. CT has been used to characterize micro-fracturing (Cnudde and Boone, 2013) and can yield three-dimensional images of micro-fractures embedded in porous rocks.

Many of the rocks in the upper crust, reaching a depth of around 50–70 km, are, in the most general, informal sense, “rigid,” and are elasto-frictional, quasi-brittle materials. A brittle rock subjected to stresses will undergo elastic deformation, but if the stress surpasses the “strength” of the rock, the rock will undergo irreversible, nonlinear deformation, leading to the creation of fractures. Numerous failure criteria have been devised to describe the triggering of fracturing due to stress concentrations, including Mohr–Coulomb (Jaeger *et al.*, 2007), Hoek–Brown (Hoek and Brown, 1980), Drucker–Prager (Drucker and Prager, 1952), Mogi (Mogi, 1971), and their generalizations, derivations, and combinations (Bigoni and Piccolroaz, 2004). However, failure of a rock is rarely caused by the propagation of a single crack; instead, it is triggered by the coalescence of multiple aligned cracks that form during deformation (Hoek and Bieniawski, 1965). Furthermore, these types of failure criteria, based on the “continuum” stresses that are implicitly averaged over lengths much greater than those of individual pores or microcracks, cannot predict the complex crack paths that originate during crack propagation due to interaction with neighboring cracks (Brace and Bombolakis, 1963).

Failure of an initially intact, brittle material is usually a two-stage process that begins with diffuse, inelastic degradation of the material, also known as “damage.” At a very small scale, damage can result from dislocations in the matrix of a crystal, localizing into micro-cracks within a grain of rock or between rock grains. Damage is followed by localization of the loss

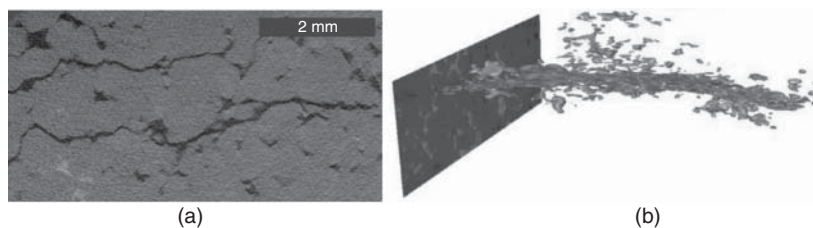


Figure 1.3 Micro-CT image of a fractured sandstone in (a), from which fracture surface can be extracted, as shown in (b), using standard segmentation techniques. Source: Iglauer *et al.* (2011) / Reproduced from John Wiley & Sons, Inc.

of integrity, leading to the growth of larger fractures. The length of “damage zones” ahead of fracture tips is a function of the grain size of the rock (Bažant and Kazemi, 1990). The size of this damage zone also depends on the heterogeneity distribution within the rock and on the influence of preexisting micro-fractures around fracture tips.

When studying fractures in the geological context, fractures are usually several orders of magnitude larger than the assumed near-tip fracture damage zone, allowing the assumption that the fracture process is a linear elastic process. The mechanical behavior of rocks can be described by idealizing the rock as a linear elastic, isotropic, and homogeneous medium, an approach that is referred to as *linear elastic fracture mechanics* (LEFM). Geological patterns such as pervasive extensional fracture patterns have been reproduced using LEFM, including fractures and faults in layered systems in two dimensions (Renshaw and Pollard, 1994; Schöpfer *et al.*, 2007) and three dimensions (Paluszny and Zimmerman, 2013), as well as single (Bremberg and Dhondt, 2009) and multiple (Paluszny and Zimmerman, 2011) fracture propagation and interaction in three dimensions.

1.3 Morphology of Single Fractures

At the millimeter scale, a rock will be composed of a few solid grains and pores. The behavior of these grains and pores can be approximated by idealized descriptions of spheres and ellipsoids, for example, using poroelasticity and effective medium theories (Zimmerman, 1991). Due to the range of grain sizes of sandstones (Boggs, 2012), at the meter scale, an intact piece of this type of rock can be expected to contain a large number of grains, pores, and additional heterogeneities. Importantly, this definition guarantees that, for a meter-scale sample, the sample size is several times larger than any individual grain of the rock. Thus, the scale at which the behavior of the constituting parts is described, and the scale at which these parts act together as a continuum, can be clearly separated. It follows that the behavior of such a rock at the meter scale will not be controlled by a single grain but by a representative number thereof. This separation of scales facilitates the derivation of governing equations that treat the ensemble of pores and solids as a continuum.

Rocks often contain a distribution of micro-heterogeneities that range from hard to soft inclusions, voids in the form of pores and vugs, micro-fractures, cemented veins, and fibers, among other features. Small-scale heterogeneities in rocks arise due to a combination of phenomena that take place during the formation of the rock and throughout its deformation and flow history. These heterogeneities can be due to the mechanical differences between the grains or crystals that initially formed the rock and their response to temperature, reactive flow, dissolution and precipitation, mineral replacement and deposition, and deformation of the rock over millions of years (Chen *et al.*, 2015). These differences lead to local stress concentrations which, when exceeding the local tensile strength of the rock, evolve into small discontinuities within and between grains, forming distributions of flaws that are present in most quasi-brittle rocks. This underlying variability has been characterized in the context of subsurface reservoir engineering, and it is now well established that it plays an important role in controlling the fluid flow and storage properties of the rock matrix.

At the meter and kilometer scales, heterogeneities can appear in the form of layers, fractures, or faults. Discrete breaks in quasi-brittle materials create discontinuities in the mechanical and fluid properties of the rock at many scales. Above the centimeter scale, discontinuities that form under tension are often referred to as “joints” or “cracks,” whereas those that form under shear are often referred to as “faults” (Jaeger *et al.*, 2007). Joints are discontinuities that have not been subjected to shear, whereas fault walls have been subjected to shear displacement. These evolve to have a variety of structures and properties; in the broadest sense, both can be regarded as “fractures.”

At smaller scales, geological materials exhibit much lower tensile strength than shear strength, and therefore, small tension fractures are ubiquitous. At larger scales, the pervasive presence of heterogeneities translates into lower shear strength, promoting the formation of large faults. Due to these two distinctions, smaller-scale tension discontinuities are often regarded as “fractures,” whereas the term “fault” is often reserved for large-scale geological discontinuities that have experienced considerable relative displacement of their walls, either due to having been formed under shear or as the result of the transition of a fracture into a fault due to changes in the regional stresses. In particular, the walls of faults will have moved parallel to the plane of the discontinuity and, in the more general sense, faults are regarded as zones with related deformation structures surrounding the discontinuity, such as secondary fractures and crushing zones (Davatzes and Hickman, 2010). Fractures and faults can form under both extensional and compressional stress regimes, and both types can be found at a range of scales. Hence, small-scale faults are frequently observed in the field, as well as large-scale fracturing that can also be observed on the Earth’s surface and on the surfaces of many other rocky and icy planets and satellites.

Multiple fractures can grow in the same direction in response to regional stresses, forming sets that, when superimposed, may form interconnected fracture networks. Growing fractures will coalesce against preexisting free boundaries or open fractures, establishing a geometric record of the relative age of the intersecting fracture sets. Thus, younger sets can be recognized, as they will be populated by shorter, more recent fractures that will have “abuted” against older, preexisting fractures. Fractures within a growing set will interact and intersect, modifying each other’s growth orientation, length, and aperture. These interactions complicate the relationship between the orientations of these fractures and the regional stresses that originally led to their growth.

Fractures and faults in the subsurface have small aspect ratios, meaning that their thickness or aperture is many times smaller than their length. Faults frequently displace layers relative to one another, whereas fractures are often restricted by geological layers and display complex cross-cutting relationships. Fractures have varying permeabilities that can either promote or restrict flow, often depending on the current stress state and possible geochemical and mechanical processes that may have affected their internal structure. Typically, fractures have a variable aperture, intersect at small angles, and range in size over several orders of magnitude. Without loss of generality, rock discontinuities in general will be referred to as “fractures” in this book. The morphology of individual fractures and fracture networks changes as the rock mass deforms due to stress. These effects are discussed further in Chapters 3 and 8.

Fracture Shape

Stand-alone fractures can be considered as planar surface inclusions in a volumetric domain. In two-dimensional cut-planes of a fractured rock mass, such as outcrops and cliffs, fractures appear as lines and sets of lines that may be planar or curved and often align and organize to form larger, organized structures. In three dimensions, fractures can be approximated by planar disks or rectangular surfaces (Adler *et al.*, 2012). Their shapes are dictated by a combination of effects, due to the medium in which they grow, and other structures with which they interact. In layered media, fractures are quick to intersect the boundaries of the rock and form rectangular shapes. When intersecting each other in layered media, fractures often create a distribution of “blocks” that effectively subdivide the rock into smaller regions.

In monolithic rocks, such as granites, fractures tend to grow unimpeded, until reaching the boundaries of other fractures or discontinuities. In these media, fractures can be approximated by low-aspect ratio, flat spheroidal or ellipsoidal inclusions that are initially disk-shaped. As they grow, shapes may become sub-planar, curved, or even shaped like complex polyhedral surfaces. Once enough fractures intersect, they may become one larger fracture, or they may intersect to the point that they fragment the rock and subdivide the rock into smaller, disconnected sub-domains.

As fractures grow, their proximity locally overwrites regional stress conditions, effectively rotating stresses around the moving crack tips. This may lead to hooking, bending, intersection, or arrest of the fracture. When fractures interact during growth, their tips may hook against another fracture, as can be seen in Fig. 1.4a. Interactions can be systematically quantified using “interaction maps” that describe the effect of relative orientation as well as distance between fractures on interaction (Thomas *et al.*, 2017).

The results of multiple numerical simulations that quantify interaction between a static fracture and a secondary fracture that is located near the first fracture are summarized in Fig. 1.4. For each location, represented by a point on the graph, the intensity of the interaction is plotted between white (no interaction) and black (strong interaction). A one-meter-long static fracture is located at the origin. Each dot represents a simulation, with a second fracture that is centered at the dot. The graph summarizes the results of eighty numerical simulations. The gray-scale values of C_{\perp} and C_{\parallel} capture the relative tensile and shear stress intensity concentration, respectively, of a system subjected to uniaxial extension, containing the static fracture and the secondary fracture (Thomas *et al.*, 2017). For tension, fractures placed to the right and above the static fracture yield the greatest interaction. For shear, the interaction is substantially lower than that in tension.

The parameter ϵ_1 (not to be confused with strain) indicates whether the relative stress measure C_{\perp} is tensile (black) or compressive (white). The plots of ϵ_1 show that in regions ahead of the tip, fractures promote each other’s growth, whereas growth in the region above the fracture is inhibited. For secondary fractures placed close to the static fracture, the magnitude of stress concentration is much higher than if placed away from the fracture. Thus, fractures aligned with each other will tend to promote each other’s growth, whereas fractures that are stacked parallel to each other will tend to inhibit each other’s growth (Thomas *et al.*, 2017).

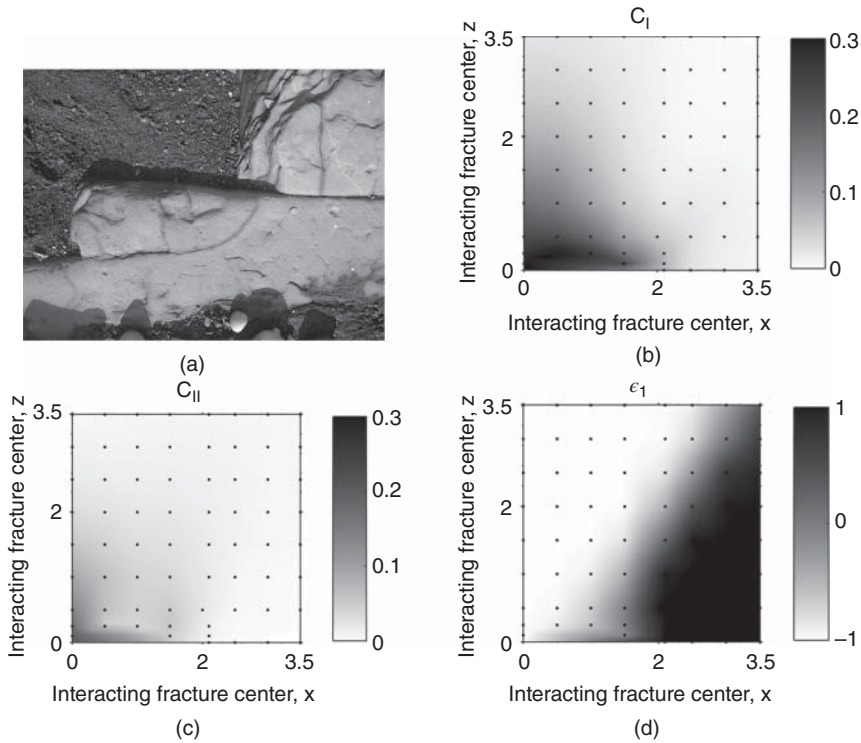


Figure 1.4 Interacting fractures. (a) A fracture hooks and coalesces with another fracture. Graphs (b) and (c) summarize the results of multiple numerical simulations that quantify interaction between a static fracture and a secondary fracture that is located near the first. The intensity of the interaction varies from no interaction (white) and strong interaction (black), quantified in terms of tensile (b) and shear (c) stresses. Dark areas in (d) show regions of tension, and light areas show regions of compression. See the text for further details.

Fracture Length

The length of a fracture is defined by the geometric extent of the curving plane that follows the fracture surface. In the two-dimensional case, fracture length is easily identified with the extent of the fracture and is also proportional to the fracture surface area. In three dimensions, the “length” must take into account the varying geometry that a fracture may present. If fractures are represented by circular disks, the length can be identified with the diameter. For fractures represented by rectangular shapes, length is defined as the measure of its longest side. For nonplanar, complex fracture shapes, length can be approximated using the definition of an equivalent radius or an equivalent extent measure, such as

$$L_f = 2\sqrt{A_f/\pi}, \quad (1.1)$$

where L_f [m] is the fracture “length” and A_f [m²] is its surface area, when the fracture is thought of as a two-dimensional surface embedded in three-dimensional space.

Observing and characterizing fracture lengths presents a challenge, both in the sub-surface and in surface outcrops. In layered media, the trace of the fracture on the rock

face is representative of its length. In other cases, such as on the face of a tunnel or the edge of a cliff, intersecting fractures can be “traced.” The trace length of a fracture is the intersection of the fracture with the wall at an arbitrary plane, and therefore its length may not be representative of the actual length of the fracture, in addition to being subject to sampling bias.

For a quasi-heterogeneous brittle material, such as most rocks, flaws and small cracks that initially approximately follow a Gaussian size distribution will concentrate stress at their tips during deformation, leading to growth. In particular, flaws with low aspect ratios (e.g., less than 0.1) will tend to grow, align, and coalesce, forming small fractures and thereby leading to even more growth. As fractures grow, their lengths differentiate further, as some fractures are subjected to substantially more growth than others. This variability in lengths is a result not only of the *in situ* and deformation stresses but also of the interaction between the fractures, faults, and other heterogeneities in the rock. It follows that fracture length distributions are usually described using length–frequency relationships. These relationships are based primarily on geological outcrop observations, as fracture lengths cannot readily be measured in boreholes, nor can they be easily interpreted using geophysical imaging, using current techniques.

Fracture length distributions from the meter up to the kilometer scale follow a power-law distribution (Barton, 1995; Bonnet *et al.*, 2001). An example of this behavior can be observed at the Forsmark site (Munier, 2004) that has been chosen for the geological disposal of nuclear waste in Sweden. Detailed fracture trace mappings of the site illustrate the pervasive nature of faults and fractures. Fractures of tens of meters in length can be identified on the scale of tunnel excavations, whereas single-kilometer-long fault discontinuities span the extent of the entire site.

The size distribution across these scales can be approximated by a power-law distribution of the form

$$f(L) = bL^{-n}, \quad (1.2)$$

where L is the fracture length (written here without the subscript f , for notational simplicity), b is a proportionality coefficient for the relationship between amount of fractures and their length, and n is an exponent, sometimes referred to as the “fractal dimension” of the network. The latter term is often used to describe the exponent, despite the fact that fractures in a network can obey a power-law size distribution without forming a fractal geometry (Munier, 2004). It follows from Eq. (1.2) that $f(L)dL$ equals the number of fractures with lengths in the range of $[L, L + dL]$. The exponent n generally varies between 1 and 3.5, with a “typical value” around 2, with factors such as stress history, linkage and connectivity, scale, and sampling bias affecting the value. The value of b , also known as the density factor, varies over a much wider range: between 10^{-3} and 10^5 for faults and between 1 and 100 for fractures, as it depends on n and on the minimum and maximum values of the fracture radii within the network (Bonnet *et al.*, 2001).

The fact that fractures are consistently observed to follow a power-law size distribution suggests that, at any scale of investigation, a single fracture could be expected to control the observed domain. This hints at a lack of separation of scales between fractures and the domain of interest, which has led to the development of numerical models that represent fractures explicitly (Cundall, 1980; Long *et al.*, 1982) rather than as part of a homogenized

continuum. This approach has been termed “discrete fracture modeling” (DFM), which indicates that fractures and intact rock are both explicitly represented and governed by separate sets of equations (*e.g.*, Geiger *et al.*, 2004).

Fracture Aperture

The aperture of a fracture, usually denoted by h [m], is a scalar quantity that reflects the physical separation between the walls of a fracture at any point in the nominal fracture plane. Apertures capture the variable distance between fracture walls along their geometry. Although many slightly different definitions of aperture have been proposed (*cf.*, Oron and Berkowitz, 1998), the simplest and basic definition is that the aperture is the distance between the two opposing fracture faces, as measured perpendicularly to the nominal fracture plane. Apertures at depth can be observed and quantified when drilling boreholes and can be measured in outcrops. Fractures that are open will increase the permeability of a rock. Fractures that are “closed,” with their walls in contact, are less permeable but still retain residual permeability, as explained in Chapter 3. Discontinuities can also seal if they are filled with mineral cement, resulting in a drastic reduction of their permeability (see Fig. 1.5a, b). The resulting veins have a thickness that reflects the aperture of the fracture at the time of precipitation (Vermilye and Scholz, 1995).

For a favorably oriented disk-shaped fracture under tension, apertures will be largest at the center and will reduce to zero at the fracture tips. Some analytical and numerical models assume that fractures have only a single aperture, which may be representative (for example, on average) of the aperture of the fracture. Some numerical models are able to capture apertures as a property that varies along the fracture surface and may change due to mechanical, thermal, or chemical changes in the rock, or due to fluid traveling through the rock (see Chapter 8). Due to the coalescence of smaller fractures into single larger fractures, as shown in Fig. 1.5a, the shape of the fracture may have variations in orientation that can translate into variations of the aperture.

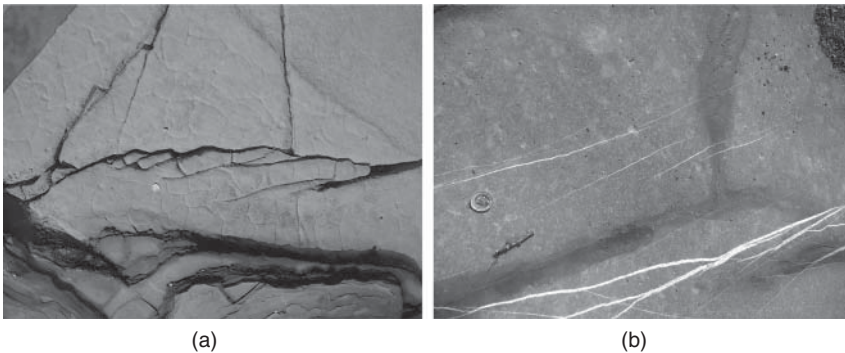


Figure 1.5 Fracture arrays. (a) Interacting fractures on a weathered rock form an array that has linked into a single larger fracture. (b) An array of fractures (top) has formed next to a larger fracture (bottom). These fractures are mineralized, and their apertures, in white, are captured by the precipitation of dissolved rock during regional deformation.

Fracture apertures, which control fracture permeability, are responsive to the history of deformation of the fracture surface and result in an uneven distribution of flow along the fracture surface in the form of channeling (Tsang and Tsang, 1989). This leads to a lower permeability of the fracture as compared to the length-dependent permeability assumption (Lang *et al.*, 2015). There are multiple factors, in addition to fracture network topology and connectivity, such as *in situ* stresses, which may strongly affect the enhancement or reduction of permeability during fracture growth and intersection (Paluszny and Matthäi, 2010).

The linear elastic deformation of the matrix predicts apertures that scale linearly with the length of the (isolated) fracture (Olson, 2003):

$$h_{\max} = \frac{(1 - \nu)\sigma}{G} L_f, \quad (1.3)$$

where h_{\max} is the maximum aperture of the fracture, σ is the effective driving stress, ν is Poisson's ratio, and G is the shear modulus of the rock matrix, which for an isotropic homogeneous material is related to the Young's modulus by $E = 2G(1 + \nu)$. The *aspect ratio* of a fracture, α [-], is usually defined by

$$\alpha = h_{\max} / L_f. \quad (1.4)$$

Measurements and simulations over multiple scales yield a log-linear distribution of aperture-length distributions (Renshaw and Park, 1997) that follow a bi-linear distribution that shifts when the length of the fracture transitions from the small to the large scale. Based on field measurements of mineralized veins and igneous dykes in the field, aperture-length relationships can be expressed as

$$h_{\max} = C(L_f)^e, \quad (1.5)$$

where C is the pre-exponential constant, which ranges from 7×10^{-4} to 0.43, and e is the power-law scaling exponent, which ranges between 0.38 and 0.41 (Olson, 2003).

This shift is not attributed to a difference in the mechanical process of fracture growth, but rather to the complexity of the heterogeneities that emerge at larger scales that affect the manner in which stress perturbations induced by larger fractures affect smaller fractures. Specifically, it is observed (Renshaw and Park, 1997) that for the small scale, when $\log(L_f) \leq \log(L_o)$, the behavior is super-linear, with $s_1 > 1$, and

$$\log(h_{\max}) = s_1[\log(L_f) - \log(L_o)] + \log(h_o), \quad (1.6)$$

where $s_1 > 1$ ranges from 1.76 to 2.54. For larger fractures, for which $\log(L_f) > \log(L_o)$, the behavior is approximately linear, with

$$\log(h_{\max}) = s_2[\log(L_f) - \log(L_o)] + \log(h_o) \approx [\log(L_f) - \log(L_o)] + \log(h_o), \quad (1.7)$$

where s_2 ranges between 0.70 and 1.28, with $\log(L_o) \in [-0.17, 1.26] \log_{10}$ -m. In addition, a sublinear relationship between length and aperture has also been reported, based on the measurement of mineralized fractures in the field. Figure 1.6 shows the length-to-aperture scaling laws that were proposed by Renshaw and Park (1997) based on various field data. The length-to-aperture ratio that corresponds to a uniform aspect ratio of 0.01 is shown, for comparison.

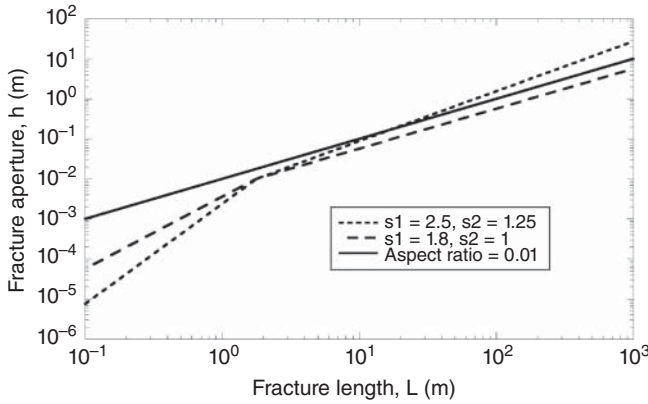


Figure 1.6 Length–aperture scaling law proposed by Renshaw and Park (1997), plotted from Eqs. (1.6) and (1.7), for the case $\{\log_{10}(L_0) = 0.25, \log_{10}(h_0) = -2\}$, for two different pairs of the parameters $\{s_1, s_2\}$. The case of a uniform aspect ratio of 0.01 is also plotted for comparison. Source: Adapted from Renshaw and Park (1997).

Fracture Surface Roughness

During their growth, fracture surfaces accrue small deviations from their original plane of nucleation. Fracture walls are not perfectly planar, and the small variations off the plane constitute the “roughness” of the fracture walls. Roughness exists at many length scales in rock fractures and can be approximated by a Gaussian height distribution and self-affine organization (Brown and Scholz, 1985). Self-affine surfaces form a fractal geometry local to the fracture surface, with statistical invariance under a scale transformation that has an anisotropic aspect ratio:

$$\Delta \mathbf{x} \rightarrow \zeta \Delta \mathbf{x}, \tag{1.8}$$

$$\Delta h \rightarrow \zeta^H \Delta h, \tag{1.9}$$

where $\Delta \mathbf{x} = (x, y)$ is the fracture in-plane coordinate vector, ζ is a constant that quantifies the magnitude of the transformation, h is the height of the fracture surface above some nominal plane, and H is the Hurst exponent, which lies between 0 and 1. The relation between the Hurst exponent, which describes the “jaggedness” of the surface, and the fractal dimension D_f of a two-dimensional surface, can be expressed as

$$H = 2 - D_f, \tag{1.10}$$

whereas for a three-dimensional surface, the relationship is

$$H = 3 - D_f. \tag{1.11}$$

Tensile fractures follow a nearly universal scaling exponent of $H \approx 0.8$, as measured for a range of different rock types and grain size distributions (e.g., Poon *et al.*, 1992). The fact that the fractal geometry is statistically invariant implies that when portions of a surface profile are magnified, the same structure becomes apparent at the smaller scale again and again (see Figs. 1.7 and 1.8).